



Journal of Advanced Research in Fluid Mechanics and Thermal Sciences

Journal homepage:

https://semarakilmu.com.my/journals/index.php/fluid_mechanics_thermal_sciences/index

ISSN: 2289-7879



Numerical Investigation of NO_x Reduction in a Hydrogen-Fueled Pulse Detonation Engine

Mahammadsalman Warimani^{1,3}, Fharukh Ahmed Ghasi Mahaboobali², Sher Afghan Khan^{3,*}, Sonachalam Muthuswamy⁴, Sayed Ahmed Imran Bellary⁴

¹ Department of Mechanical Engineering, P.A. College of Engineering, Mangalore, Karnataka, 574153, India

² Government Engineering College, Huvinahadagali, Vijayanagar District, Karnataka, 583219, India

³ Department of Mechanical & Aerospace Engineering, Faculty of Engineering, IUM, Gombak Campus, Kuala Lumpur, Malaysia

⁴ Department of Mechanical Engineering, Arvind Gavali College of Engg, Satara, Maharashtra, 415015, India

ARTICLE INFO

Article history:

Received 21 October 2023

Received in revised form 18 January 2024

Accepted 2 February 2024

Available online 29 February 2024

Keywords:

Pulse detonation engine; EINO_x; CFD; performance characteristics

ABSTRACT

A change in combustion concepts from conventional isobaric to constant volume combustion (CVC) has several advantages. Pulse detonation combustion (PDC) operates on CVC, increasing the engine's thermodynamic efficiency significantly. Little research has been conducted on pollutant emissions from pulse detonation engines (PDE). Because PDE burns at a higher temperature, it emits more NO_x. The formation of NO_x is investigated in this paper using the computational fluid dynamics (CFD) method. For hydrogen fuel, a model is built by varying pressure, temperature, spark size, and geometry. The SST K- ω model is used with transient conditions. EINO_x was calculated using CFD analysis for 12 cm and 20 cm tubes. The results were encouraging. A 12 cm tube produced 200 g/kg of fuel EINO_x, while a 20 cm tube produced 250 g/kg of fuel EINO_x. The computed results are consistent with previous literature.

1. Introduction

It is necessary to find a more efficient thermodynamic engine. Numerous studies have been conducted to more efficiently harness energy [1]. It is necessary to find an engine that has higher thermodynamic efficiency. A pulse detonation engine (PDE) operates like the Humphrey cycle, which is based on constant volume combustion and has a higher thermodynamic efficiency than gas turbines. High pressures and temperatures within the detonation wave, on the other hand, indicate increased emissions [2]. Nitrogen oxides (NO_x) are produced in PDE due to higher combustion temperatures. The production of nitrogen oxides (NO_x) during the combustion of fuels with air causes significant environmental damage. NO_x emissions, which include the gases nitric oxide (NO) and nitrogen dioxide (NO₂), contribute to ozone depletion, cause photochemical smog, and endanger

* Corresponding author.

E-mail address: sakhan@ium.edu.my

<https://doi.org/10.37934/arfmts.114.2.106117>

human health and the stratospheric protective ozone layer [3,4]. As a result, it is necessary to investigate NO_x emissions caused by PDE and potential ways to reduce them.

Few researchers have previously studied PDE for emission analysis. Researchers such as Yungster and Breisacher investigated the formation of NO_x in hydrocarbon-fueled PDE numerically and experimentally. The results show that operating with lean or rich mixtures and using the shortest possible detonation tubes reduces NO_x formation in Jet-A-fueled PDEs [5]. Djordjevic *et al.*, [6] used three primary methods for hydrogen fuel: lean combustion mixtures, dilution by steam injection, and exhaust gas recirculation. The results show that nitrogen dilution, simulating external recirculation of the cooled exhaust gas, could achieve higher NO_x reduction than steam injection. Djordjevic *et al.*, [6] experimented to assess the impact of parameters such as operating frequency, sample time, fill time, pulse detonation combustion exit, and probe geometry on NO_x emission. It was discovered that determined NO_x emissions can vary significantly depending on the factors chosen. Xisto *et al.*, [7] discovered that detonation in lean mixtures significantly reduced NO_x emissions. Frolov [8] discovered that nitrogen oxide emissions from detonation burner units (DBUs) are significantly lower than those from powerful conventional burners with comparable characteristics. It is well known that PDE has very complex phenomena such as strong shock wave formation, and the turbulent nature of flow makes experimental methods difficult to predict emission. One of the biggest issues in the thermonuclear and petrochemical industries today is flow regime identification, which is crucial to the efficient operation of facilities for the processing and transportation of multiphase fluids [9]. Computational fluid dynamics (CFD) can, however, solve problems associated with experimental work [10].

Schauer *et al.*, [11] discovered that nitric oxide formation peaks around 0.9 and decreases at higher and lower equivalence ratios. Fill fractions of less than one result in increased oxygen consumption and decreased nitric oxide emissions. Sudarja and Sukamta [12] found out the two-phase flow characteristics of the low surface tension liquid and gas, namely the void percentage and flow regime. According to Garan and Djordjevic [13], this study applies conventional NO_x-reducing measures to a pulse detonation combustor in multi-cycle operation, such as fuel-lean mixtures and nitrogen dilution (emulating exhaust gas recirculation), in some cases, water also used to enhance the heat transfer so that reduced the NO_x emission [14]. Their influence on the composition of exhaust gases is measured and compared to numerical predictions made by two available simplified models.

The manuscript by Anand and Gutmark [15] is dedicated to reviewing the emissions characteristics of four major types of sure gain combustors PGCs: wave rotor combustors, pulsejets, pulse detonation combustor (PDC), and rotating detonation combustors RDCs. The literature on NO_x emissions caused by PDE is limited. As a result, the motivation for the current study is to gain insight into the effect of flame temperature on emission using CFD methods for hydrogen fuel. The CFD investigation in this article looked at emissions from hydrogen-fueled PDE with different parameters like geometry, pressure, temperature, and spark gap of the PDE tube. To the best of the authors' knowledge, this is the first attempt to use the analytical method to find EINO_x for blended fuels.

2. Methodology

2.1 Computational Domain

In computational fluid dynamics (CFD), two different sizes of detonating tubes are chosen. They have dimensions of 20 cm, 12 cm, and the same diameter of 2 cm, as shown in Figure 1. The geometric model was created with the ANSYS fluent software. It is axisymmetric in two dimensions. The geometry size of 200 mm is similar to that used by Bussing and Pappas [16] and Morris [17]. In these

computations, a small spark area is used to start the detonation, as shown in Figure 2. Because it is symmetrical about the x-axis, only the upper half of the PDE geometry will be studied for this study.

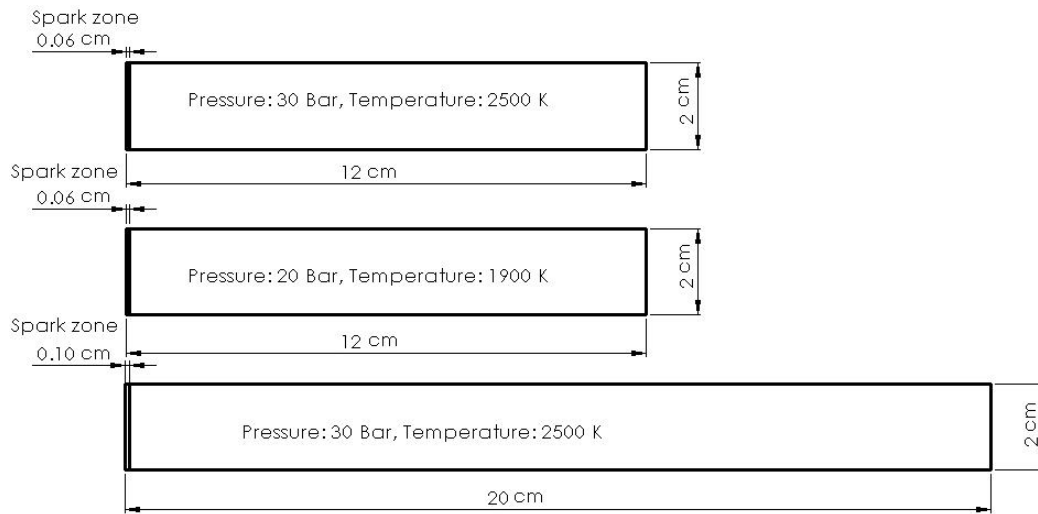


Fig. 1. Model geometry

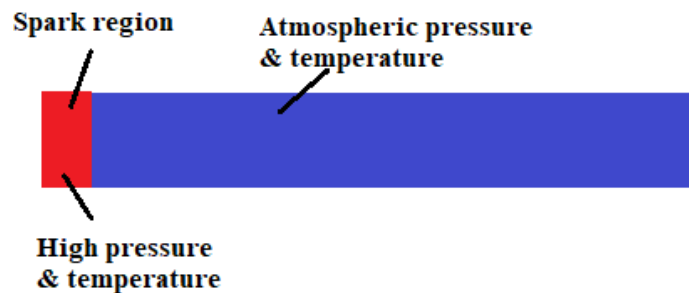


Fig. 2. High pressure and temperature patch

2.1.1 Mesh independence analysis

High-fidelity simulation is inspected by varying mesh sizes. Initially, the study of the detonation tube began with 40000 elements to save computational time. Once the track-matching results became the same as the values obtained in the previous literature and NASA CEA, the grid size gradually increased. This was scrutinized to eliminate the error that occurred in various mesh sizes. As shown in Figure 3, grid sizes of 60000 (mesh1), 80000 (mesh2), and 100000 (mesh3) elements were selected. The detonation velocity of 2040 m/s, 2280 m/s, and 2300 m/s were produced by mesh 1, mesh 2, and mesh 3, respectively. In the grid size of 0.1 million elements, the detonation velocity error is minimal compared to 80000 elements. Thus, the simulation results shown in this paper have 0.1 million element sizes. Varying mesh sizes investigate error analysis of results. By considering mesh 1 and mesh 2, the error in terms of detonation velocity is 10.52 %. So, to reduce the error percentage, mesh 3 is considered. The error percentage between mesh 2 and 3 is 0.86%, which is considerably less than mesh 1. As a result, it was concluded that a mesh 3 that is the size of 0.1 million elements was suitable for numerical computations [18].

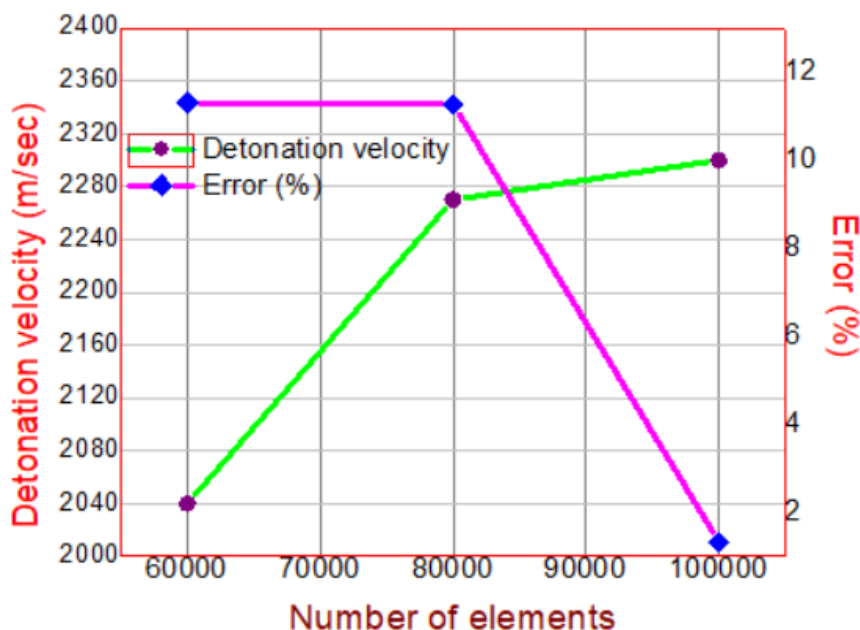


Fig. 3. PDE tube graph for grid convergence test

2.2 Boundary Conditions

The boundary conditions of the PDE tube are shown in Figure 4. This 2-D axisymmetric simulation's computational region was dominated by the boundary conditions wall and pressure outlet [19]. The ignition chamber is where combustion takes place. The right side of the combustion chamber is considered open, and a fixed pressure outlet boundary condition is used. The upper and left halves of the tube are considered walls.

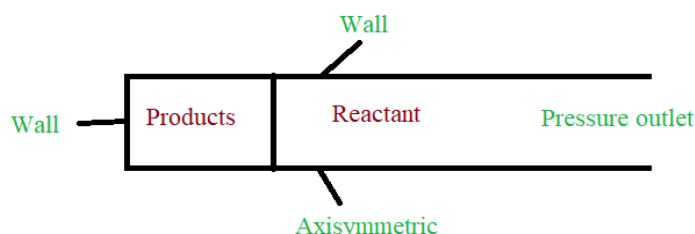


Fig. 4. The PDE tube's boundary condition

PDE is a computationally time-consuming chemically reactive flow solution. The simulation was performed on various geometric sizes of the tube-like tube length of 12 cm and 20 cm to determine the time required for simulation and whether or not detonation occurs in the selected geometry. A detonation wave can be generated with only a 12 cm geometry for hydrogen fuel.

In PDE, there are two types of initiation methods. They are direct initiation and deflagration to detonation (DDT). DDT necessitates the placement of obstacles in the tube. The direct initiation technique was used in this investigation due to DDT limitations, such as the requirement of an impractical amount of energy for direct detonation initiation in flight vehicles. The direct initiation strategy, most recently used by Xisto *et al.*, [7] is also used in this study. The placement of the spark near the closed end of the tube is critical for simulation because Detonation requires a specific amount of energy to initiate and sustain the reaction. At low temperatures, the kinetic energy of the molecules is reduced, making obtaining the activation energy required for detonation more difficult. The tube will not have the ability to detonate. This investigation looks into various spark location

sizes up until detonation. If the detonation parameters for the duration of the simulation are the same as those previously explained in the literature, the spark size from the earlier literature is chosen. Pressure and temperature are higher in the spark zone than elsewhere in the tube. If detonation has not yet been detected in the spark region, it is possible to increase the area's size, temperature, or pressure until it is the maximum area, temperature, and pressure can be varied until 400mm, 40 bar, and 4500 K. According to Kailasanath *et al.*, [20], the size, pressure, and temperature of the spark area can be varied until detonation occurs. The gaseous blend product is placed in the spark area to prevent combustion.

Flow is investigated in this study by taking into account supersonic and compressible flow. This type of problem can be solved with a density-based solver. The finite volume discretization technique is used to solve the governing equations for mass, momentum, energy, and species transfer.

At convergence, the following conditions must be met: With each iteration, the solution is no longer changing. It is possible to achieve overall mass, momentum, energy, and scalar balances. To a specified tolerance, all equations (momentum, energy, etc.) are obeyed in all cells. Monitoring convergence using residual history: In general, a three-order-of-magnitude decrease in residuals indicates at least qualitative convergence. The major flow features should be established at this point. The governing equations were continuously solved in all scenarios in this study until the residual magnitude was less than 10^{-4} . Because PDE is a high Mach number flow, Roe's Flux-Difference Splitting (Roe-FDS) was used in this study. This study compares two interpolation methods. They are first-order and second-order upwind, respectively. In this study, the standard initialization method is used. The literature indicates that detonation has a short reaction time; thus, the grid size was small the step size was 10^{-8} seconds, and the Courant-Friedrichs-Lewy (CFL) number was reduced to 0.6. For simulation, the SST k-Omega model is used. Finally, results are obtained by performing as many iterations as necessary to solve the problem in the solver.

2.3 Combustion Modeling

For CFD analysis, the composition of unreacted and reacted mixtures must be determined using the equation, and mixture reactions must be calculated using Eq. (1). In this study, the stoichiometric ratio is regarded as one. The chemical kinetics reaction balance equations were as follows:



where $a = x + (y/4)$.

The left-hand and right-hand equations must be modified to achieve balance. Eq. (2) is used to calculate the mass fraction of each composition.

$$Y = \frac{m_{fuel}}{m_{oxidizer}} \quad (2)$$

Temperature, pressure, and residence time all influence thermal NOx. As a result, the PDE tube was tested in this simulation by varying pressure, temperature, and spark zone gap. As previously stated, the detonating tube sizes chosen for the evaluation are 200 mm long, 20 mm in diameter, and 120 mm long, 20 mm in diameter. Only hydrogen fuels are subjected to PDE testing. Only the ANSYS FLUENT default available mechanisms are used. Pressure, temperature, and spark gaps are all

set so that the selected combination produces a detonation wave and detonation velocity, as described in previous literature. The geometry in this study is 2-D axisymmetric.

As shown in Table 1, different combinations are chosen for PDE analysis. In the spark zone, pressure and temperature are chosen to produce detonation waves and the required velocity. The SST k-omega model was used to analyze PDE for thermal NOx in this section.

Table 1

Summary of selected combinations for thermal NOx analysis simulation

| Pressure (Bar) | Geometry (LXD) | Spark zone (cm) | Temperature (K) | Case No |
|----------------|----------------|-----------------|-----------------|---------|
| 30 | 12X2 | 0.06 | 2500 | 1 |
| 20 | 12x2 | 0.06 | 1900 | 2 |
| 30 | 20x2 | 0.1 | 2500 | 3 |

3. Results

This research began with a look at the fundamental principles of tube detonation using hydrogen fuel. Air serves as the oxidizer in CFD analysis. One-step chemistry was used in this investigation. The investigation then compared detonation parameters with NASA CEA and published literature.

Table 2 shows the velocity results obtained from previous literature and NASA CEA for hydrogen fuel. In previous literature, detonation velocity ranged from 1965 to 2400 m/s. These variations are determined by the initial conditions chosen. Based on previous research, an average detonation velocity of 2177 m/s was calculated. Detonation velocity was achieved in this study between these published values.

Table 2

NASA CEA and the literature are used to validate the current computational model

| Parameter | Yungster <i>et al.</i> , [21] | Taylor <i>et al.</i> , [22] | Maciel and Marques [23] | Warimani <i>et al.</i> , [18] | NASA CEA |
|----------------|-------------------------------|-----------------------------|-------------------------|-------------------------------|----------|
| Velocity (m/s) | 2400 | 2020 | 1996 | 2300 | 1964.9 |

3.1 Effect of Initial Conditions

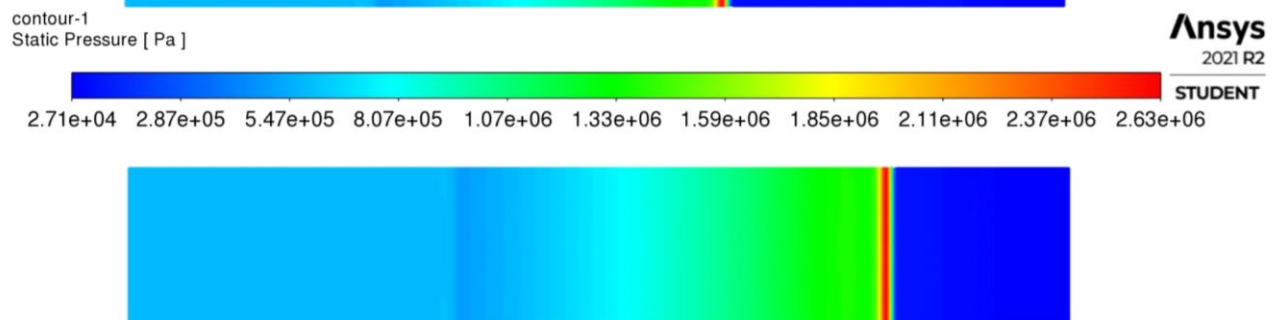
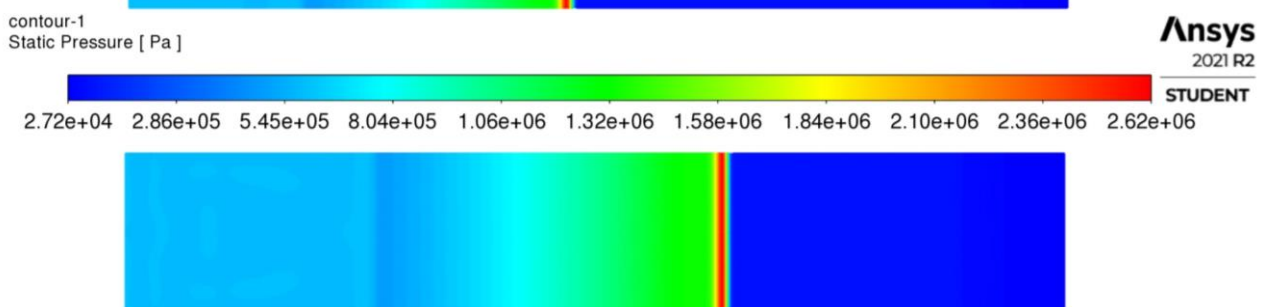
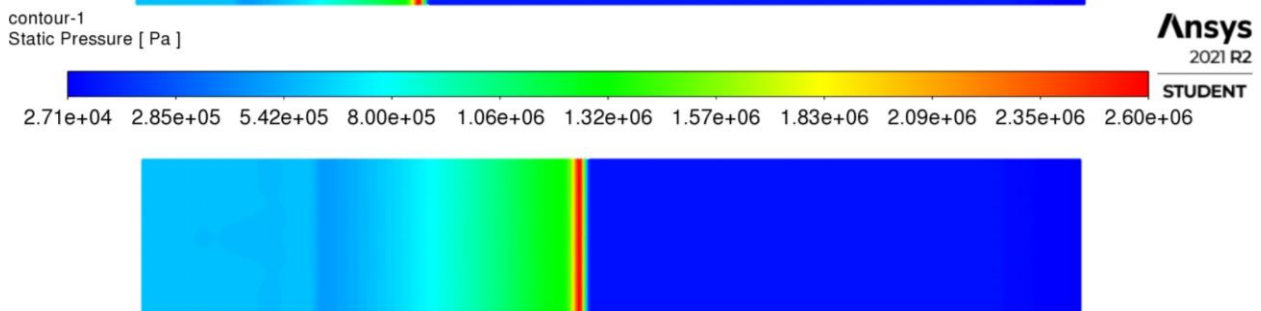
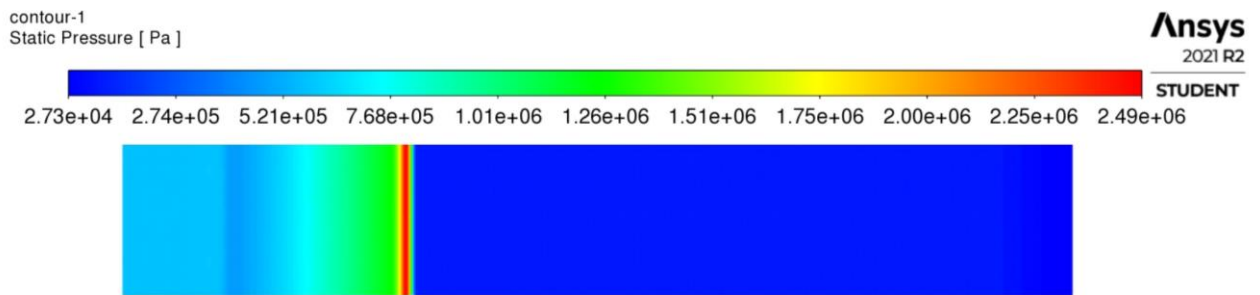
The detonation velocity for hydrogen fuel with varying initial conditions is shown in Table 3. The velocity of detonation is calculated at various points along the tube until it reaches the end. Table 3 displays the detonation velocities at the tube's end. The CFD detonation velocity value in all three cases is determined by the initial conditions. If the initial pressure, temperature, and spark size variables change, the detonation velocity changes. The varying chemical kinetics that fuels exhibit based on molecular weight and other physical and chemical characteristics cause detonation velocity to vary. As shown in Table 2, for the same pressure and temperature mixture, the detonation velocity changed for each case due to variations in tube length and spark zone size. Pressure, temperature, and spark size varied depending on the spark zone. In the case of hydrogen fuel requires little ignition energy, it has a fast flame. Because of these characteristics, hydrogen-filled small tubes can generate a higher velocity value. In our study, we chose 12 cm and 20 cm tubes for detonation combustion. In the direct initiation method, spark size is also important in generating detonation velocity. Hydrogen requires only 0.5% (0.005 length) of the size of the spark zone to generate detonation velocity. This research found that hydrogen 30 bar pressure and 2500 K temperature produced accurate results when compared to NASA CEA and available literature.

Table 3

Variation of detonation velocity and initial conditions for selected fuel

| Fuel | Pressure (Bar) | Temperature (K) | Length (cm) | Spark size (cm) | Detonation velocity (m/s) |
|----------|----------------|-----------------|-------------|-----------------|---------------------------|
| Hydrogen | 30 | 2500 | 12 | 0.06 | 2300 |
| Hydrogen | 20 | 1800 | 12 | 0.06 | 1900 |
| Hydrogen | 30 | 2500 | 20 | 0.1 | 1950 |

Figure 5 and Figure 6 show the pressure and temperature contours for hydrogen fuel in a 20 cm detonation tube. A detonation wave must be generated in at least 20 microseconds. These pressure and temperature contours are similar to standard ZND structures for hydrogen fuel. At 20 microseconds, Von Neumann's pressure spike value for hydrogen is approximately 33 bar, and the temperature is 3400 K. The pressure and temperature values obtained are consistent with NASA CEA and available literature. The same pressure and temperature values are obtained by applying the same initial conditions as described in the previous literature [21].



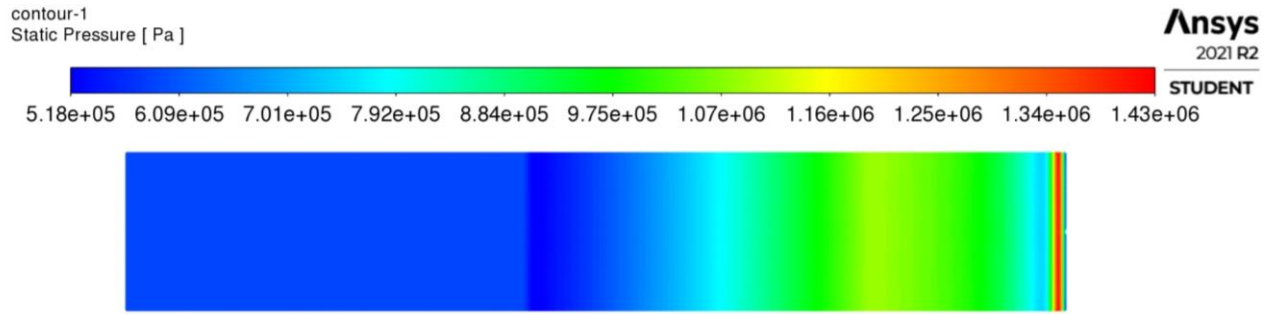
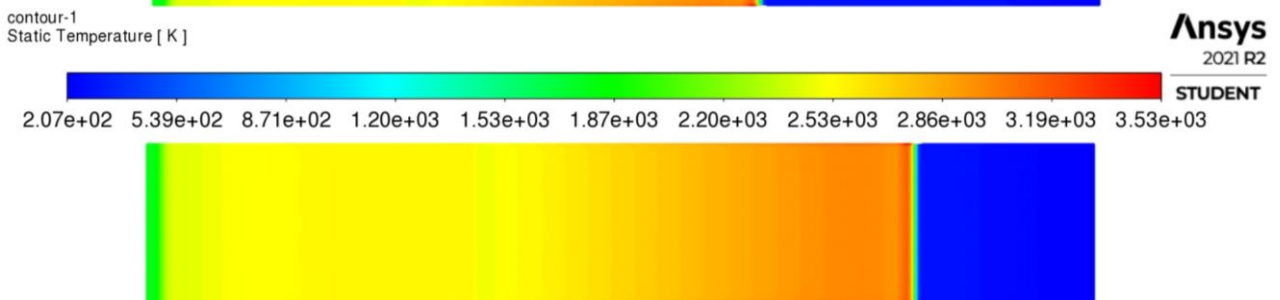
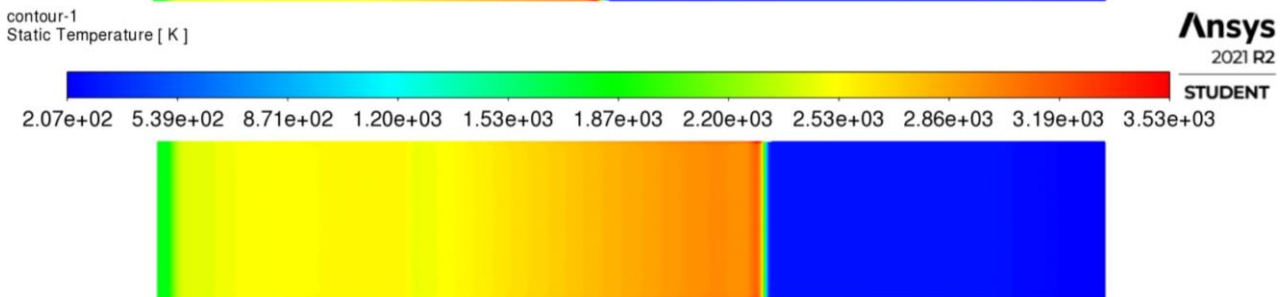
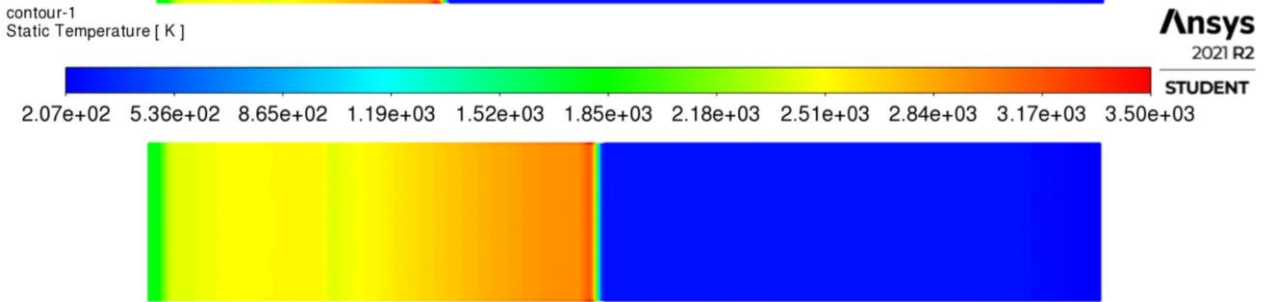
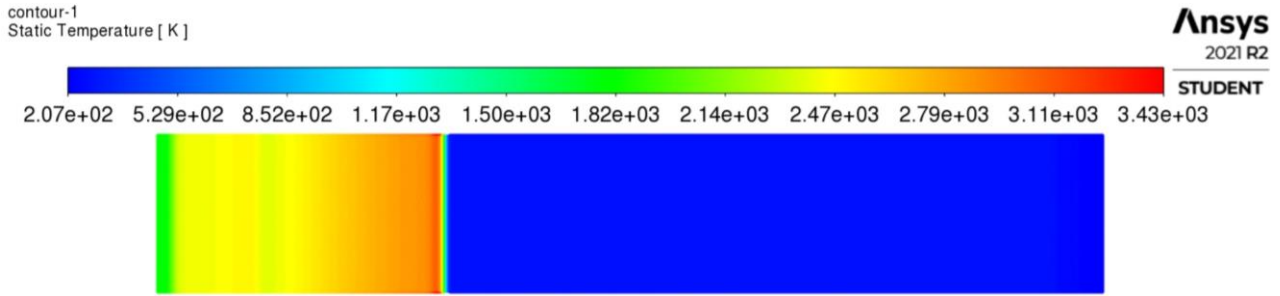


Fig. 5. Variation of pressure contour from 20 to 60 micro sec for hydrogen fuel



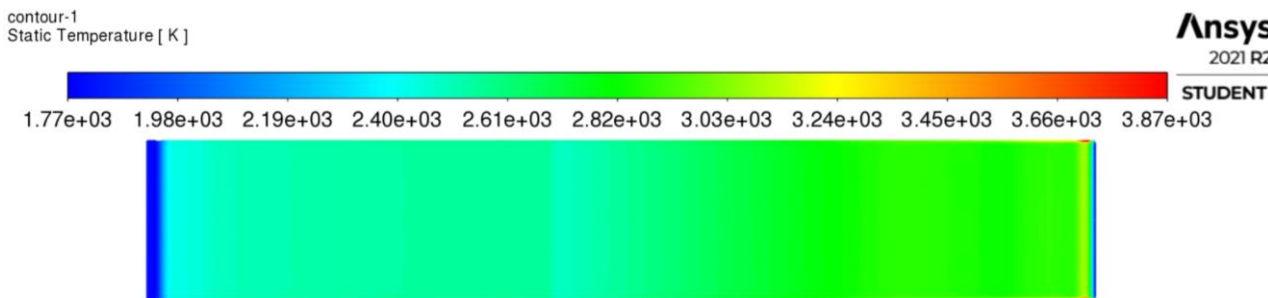


Fig. 6. Variation of temperature contour from 20 to 60 micro sec for hydrogen fuel

3.2 Comparing Emission of PDE With RAMJET Engines

Figure 7 compares the NOx emission index of the pulse detonation engine to that of supersonic transporters (SST) equipped with RAM jets. In both cases, hydrogen is used as a fuel. RAM-jets produced approximately 100 g/kg of EINOx at 10 microseconds and 656 g/kg of EINOx at 100 microseconds.

This study considers three cases of hydrogen fuel. There are two types of 12 cm tubes and two types of 20 cm tubes to consider. At 10 microseconds, two 12 cm varieties produced 50 g/kg of fuel EINOx, and the detonation tube reached the tube end at 50 microseconds. As a result, only results up to 50 microseconds are displayed. It produced EINOx of 200 g/kg of fuel in 50 microseconds. Similarly, at 10 microseconds, the 20 cm PDE tube produced the same amount of EINOx as the 12 cm PDE tube, but it produced around 250 g/kg of fuel in the end. This 20 cm PDE tube is comparable to Ramjet conditions and thus compared to it. EINOx increased mid-tube in all pulse detonation tube cases [24]. When compared to RAM jets, PDE produced significantly less EINOx. This paper is the first to compare the emission of PDE and Ramjet. With shorter tubes, the residence time over the Taylor wave and plateau region decreases, resulting in a decrease in EINOx concentration. According to previous experimental and simulation work, PDE proved that short tubes produce less EINOx than longer tubes.

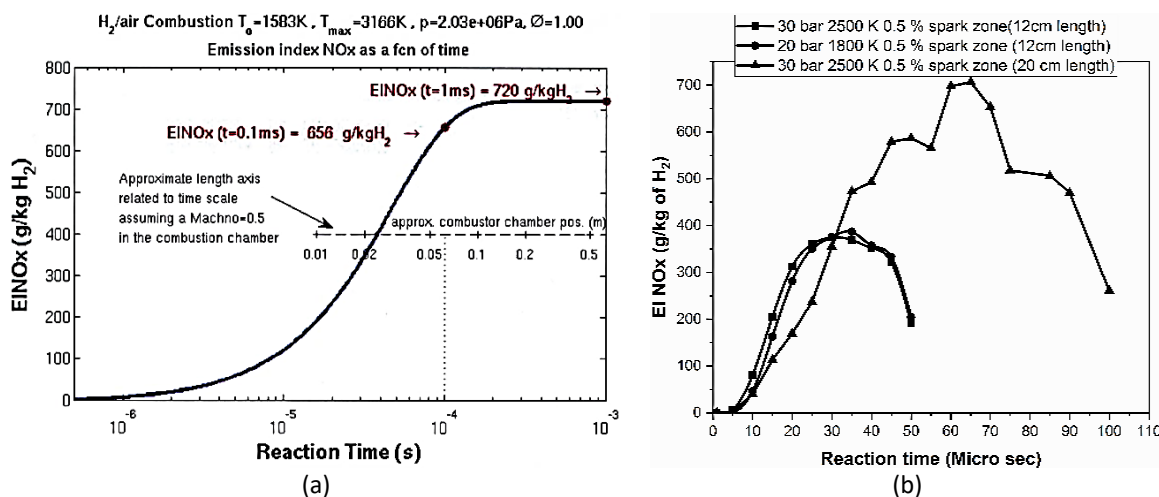


Fig. 7. EINOx comparison between RAM Jets and the pulse detonation tube of this research, (a) RAM Jets, (b) PDE [25]

Figure 8 depicts the mass fraction of pollutant number contour at the start of hydrogen fuel detonation. The goal of this analysis is to demonstrate that shorter tubes produce a lower mass fraction than longer tubes. The mass fraction results for hydrogen fuel are shown in images one

through three. Images 1 and 3 show shorter and longer tubes, respectively. Image 1 produced a lower mass fraction (0.008) because it is a shorter tube; as shown in image 3, it produced a higher mass fraction (0.009)—more mass fraction of pollutant NO produced by a longer tube than a shorter one [26]. In the meantime, images 1 and 2 show the same tube size but different temperatures. Because Image 1 has a lower temperature value, it produced a higher mass fraction than image 2. The mass fraction is justified by image 1, 2, 3 of Figure 8 because it is affected by tube size and temperature [27].

Because we used the default single-step mechanisms available in Ansys Fluent software, the results of the mass fraction of pollutant NO differ from other PDE research [28].

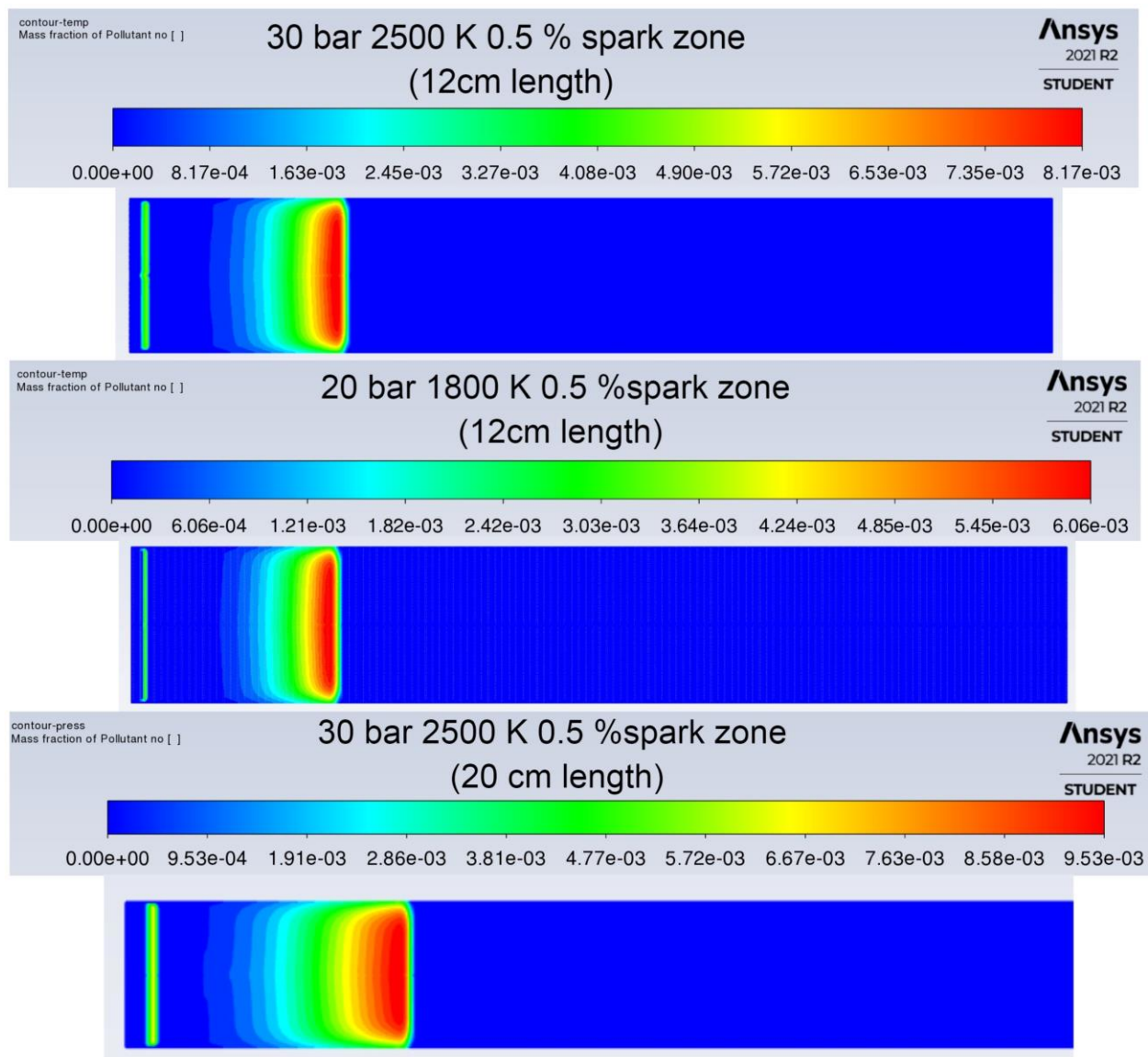


Fig. 8. Mass fractions of pollutant number contour at the beginning of detonation for hydrogen and kerosene

4. Conclusions

In the CFD investigation of emission models, it was demonstrated that for hydrogen, 30 bar pressure, 2500 K temperature, and a spark gap of 0.5% of the length produced accurate results when compared to the available literature. RAM-jets produced approximately 100 g/kg of fuel at 10 microseconds, while PDE produced 50 g/kg of EINOx fuel.

NOx measurements in a hydrogen-fueled PDE show that NOx formation is strongly influenced by temperature, spark zone gap, and fuel. These simulations agree with the experimental data fairly well. Compared with RAM-jets for hydrogen fuel, PDE produced a considerably low amount of EINOx. According to previous experimental and simulation work, short tubes produce less EINOx than longer tubes in PDE. The amount of EINOx produced in the engine is heavily influenced by the mechanisms used in the CFD analysis.

Acknowledgment

This research was not funded by any grant.

References

- [1] Umar, Hamdani, Teuku Muhammad Kashogi, Sarwo Edhy Sofyan, Razali Thaib, and Akram Akram. "CFD Simulation of Tesla Turbines Performance Driven by Flue Gas of Internal Combustion Engine." *Journal of Advanced Research in Applied Mechanics* 98, no. 1 (2022): 1-11. <https://doi.org/10.37934/aram.98.1.111>
- [2] Schwer, Douglas A., and Kailas Kailasanath. "Characterizing NOx emissions for air-breathing rotating detonation engines." In *52nd AIAA/SAE/ASEE Joint Propulsion Conference*, p. 4779. 2016. <https://doi.org/10.2514/6.2016-4779>
- [3] Hinrichs, Jörn, Maximilian Hellmuth, Felix Meyer, Stephan Kruse, Marco Plümke, and Heinz Pitsch. "Investigation of nitric oxide formation in methane, methane/propane, and methane/hydrogen flames under condensing gas boiler conditions." *Applications in Energy and Combustion Science* 5 (2021): 100014. <https://doi.org/10.1016/j.jaecs.2020.100014>
- [4] He, Zhuohui J., Clarence Chang, and Caitlin Follen. "NOx emissions performance and correlation equations for a multipoint LDI injector." In *53rd AIAA Aerospace Sciences Meeting*, p. 0098. 2015. <https://doi.org/10.2514/6.2015-0098>
- [5] Yungster, Shaye, and Kevin Breisacher. "Study of NOx formation in hydrocarbon-fueled pulse detonation engines." In *41st AIAA/ASME/SAE/ASEE Joint Propulsion Conference & Exhibit*, p. 4210. 2005. <https://doi.org/10.2514/6.2005-4210>
- [6] Djordjevic, Neda, Niclas Hanraths, Joshua Gray, Phillip Berndt, and Jonas Moeck. "Numerical study on the reduction of NOx emissions from pulse detonation combustion." *Journal of Engineering for Gas Turbines and Power* 140, no. 4 (2018): 041504. <https://doi.org/10.1115/1.4038041>
- [7] Xisto, Carlos, Olivier Petit, Tomas Grönstedt, and Anders Lundblad. "Assessment of CO₂ and NOx emissions in intercooled pulsed detonation turbofan engines." *Journal of Engineering for Gas Turbines and Power* 141, no. 1 (2019): 011016. <https://doi.org/10.1115/1.4040741>
- [8] Frolov, S. M. "Liquid-fueled, air-breathing pulse detonation engine demonstrator: operation principles and performance." *Journal of Propulsion and Power* 22, no. 6 (2006): 1162-1169. <https://doi.org/10.2514/1.17968>
- [9] Khan, Umair, William Pao, Nabihah Sallih, and Farruk Hassan. "Flow Regime Identification in Gas-Liquid Two-Phase Flow in Horizontal Pipe by Deep Learning." *Journal of Advanced Research in Applied Sciences and Engineering Technology* 27, no. 1 (2022): 86-91. <https://doi.org/10.37934/araset.27.1.8691>
- [10] Yungster, S., K. Radhakrishnan, and K. Breisacher. "Computational study of NOx formation in hydrogen-fuelled pulse detonation engines." *Combustion Theory and Modelling* 10, no. 6 (2006): 981-1002. <https://doi.org/10.1080/13647830600876629>
- [11] Schauer, Frederick, Royce Bradley, Viswanath Katta, and John Hoke. "Emissions in a pulsed detonation engine." In *47th AIAA Aerospace Sciences Meeting Including the New Horizons Forum and Aerospace Exposition*, p. 505. 2009. <https://doi.org/10.2514/6.2009-505>
- [12] Sudarja, Sudarja, and Sukamta Sukamta. "Experimental Study on Flow Pattern and Void Fraction of Air-Water and 3% Butanol Two-Phase Flow in 30° Inclined Mini Channel." *Journal of Advanced Research in Experimental Fluid Mechanics and Heat Transfer* 1, no. 1 (2020): 11-20.
- [13] Garan, Niclas, and Neda Djordjevic. "Experimental and low-dimensional numerical study on the application of

- conventional NOx reduction methods in pulse detonation combustion." *Combustion and Flame* 233 (2021): 111593. <https://doi.org/10.1016/j.combustflame.2021.111593>
- [14] Latib, Muhammad Azamuddin, and Natrah Kamaruzaman. "Simulation Study on the Heat Performance of Different Nanofluids for Rotating Detonation Engine Cooling." *Journal of Advanced Research in Micro and Nano Engineering* 5, no. 1 (2021): 1-8.
- [15] Anand, Vijay, and Ephraim Gutmark. "A review of pollutants emissions in various pressure gain combustors." *International Journal of Spray and Combustion Dynamics* 11 (2019): 1756827719870724. <https://doi.org/10.1177/1756827719870724>
- [16] Bussing, T., and George Pappas. "An introduction to pulse detonation engines." In *32nd Aerospace Sciences Meeting and Exhibit*, p. 263. 1994. <https://doi.org/10.2514/6.1994-263>
- [17] Morris, C. I. "Numerical modeling of single-pulse gasdynamics and performance of pulse detonation rocket engines." *Journal of Propulsion and Power* 21, no. 3 (2005): 527-538. <https://doi.org/10.2514/1.7875>
- [18] Warimani, Mahammasalman, Muhammad Hanafi Azami, Sher Afghan Khan, Ahmad Faris Ismail, Sanisah Saharin, and Ahmad Kamal Ariffin. "Internal flow dynamics and performance of pulse detonation engine with alternative fuels." *Energy* 237 (2021): 121719. <https://doi.org/10.1016/j.energy.2021.121719>
- [19] Harish, H. V., Birlie Fekadu, and Manjunath K. "Numerical Studies on Thermo-Hydraulic Characteristics of Turbulent Flow in a Tube with a Regularly Spaced Dimple on Twisted Tape." *CFD Letters* 13, no. 8 (2021): 20-31. <https://doi.org/10.37934/cfdl.13.8.2031>
- [20] Kailasanath, K., G. Patnaik, and C. Li. "The flowfield and performance of pulse detonation engines." *Proceedings of the Combustion Institute* 29, no. 2 (2002): 2855-2862. [https://doi.org/10.1016/S1540-7489\(02\)80349-2](https://doi.org/10.1016/S1540-7489(02)80349-2)
- [21] Yungster, Shaye, K. Radhakrishnan, and K. Breisacher. "Computational and experimental study of NOx formation in hydrogen-fueled pulse detonation engines." In *40th AIAA/ASME/SAE/ASEE Joint Propulsion Conference and Exhibit*, p. 3307. 2004. <https://doi.org/10.2514/6.2004-3307>
- [22] Taylor, Brian, David Kessler, Vadim Gamezo, and Elaine Oran. "The influence of chemical kinetics on the structure of hydrogen-air detonations." In *50th AIAA Aerospace Sciences Meeting including the New Horizons Forum and Aerospace Exposition*, p. 979. 2012. <https://doi.org/10.2514/6.2012-979>
- [23] Maciel, E. C., and C. S. T. Marques. "2-D simulation with OH* kinetics of a single-cycle pulse detonation engine." *Journal of Applied Fluid Mechanics* 12, no. 4 (2019): 1249-1263. <https://doi.org/10.29252/jafm.12.04.29593>
- [24] Warimani, Mahammasalman, Sher Afghan Khan, Sayed Ahmed Imran Bellary, Noor Alam, and Sonachalam Muthuswamy. "Analytical Evaluation of Loss Mechanism Effects on PDE Performance with Variation of Refilling Beta Parameters." *Journal of Advanced Research in Fluid Mechanics and Thermal Sciences* 109, no. 2 (2023): 66-78. <https://doi.org/10.37934/arfmts.109.2.6678>
- [25] Tengzelius, Ulf. *NOx Emissions and Engine Performance Results for Studied Engine Concepts Including Final Summary*. Defence & Security, Systems and Technology, Swedish Defence Research Agency (FOI), 2010.
- [26] Sonachalam, M., and V. Manienyan. "Optimization of critical angle, distance and flow rate of secondary fuel injection in DI diesel engine using computational fluid dynamics." *SN Applied Sciences* 3 (2021): 1-13. <https://doi.org/10.1007/s42452-020-04138-3>
- [27] Muthuswamy, Sonachalam, and Manienyan Veerasigamani. "Impact of secondary fuel injector in various distance on direct injection diesel engine using acetylene-bio diesel in reactivity controlled compression ignition mode." *Energy Sources, Part A: Recovery, Utilization, and Environmental Effects* (2020): 1-15. <https://doi.org/10.1080/15567036.2020.1810177>
- [28] Djordjevic, Neda, Niclas Hanraths, Joshua Gray, Phillip Berndt, and Jonas Moeck. "Numerical study on the reduction of NOx emissions from pulse detonation combustion." *Journal of Engineering for Gas Turbines and Power* 140, no. 4 (2018): 041504. <https://doi.org/10.1115/1.4038041>